Petroleum Research 11 (2026) 441–450

Contents lists available at ScienceDirect

Petroleum Research

journal homepage: http://www.keaipublishing.com/en/journals/petroleum-research/

Full Length Article

Synergizing foam stability, gas mobility control, and oil recovery: A new approach combining silane-silica oxide and MFomax

Mohammed Falalu Hamza [a,b,c,*], Hassan Soleimani [a,d], Bashir Abubakar Abdulkadir [e], Saifullahi Shehu Imam [b], Sabiha Hanim Saleh [c], Yarima Mudassir Hassan [f]

[a] *Institute of Hydrocarbon Recovery, Universiti Teknologi PETRONAS, 32610 Bandar Seri Iskandar, Perak Darul Ridzuan, Malaysia*
[b] *Department of Pure & Industrial Chemistry, Bayero University, Kano, 3011 Kano, Nigeria*
[c] *School of Chemistry & Environment, Faculty of Applied Sciences, Universiti Teknologi MARA, Shah Alam, Selangor, Malaysia*
[d] *Department of Geosciences, Universiti Teknologi PETRONAS, Tronoh, Bandar Seri Iskandar, 32610, Perak, Malaysia*
[e] *Centre for Research in Advanced Fluid & Processes, Universiti Malaysia Pahang Al-Sultan Abdullah, Lebuh Persiaran Tun Khalil Yaakob, Gambang, 26300, Pahang, Malaysia*
[f] *Department of Computer Science, Azman University Kano, 713140 Kano, Nigeria*

A R T I C L E I N F O

Article history:
Received 16 April 2025
Received in revised form 16 September 2025
Accepted 28 September 2025
Available online 4 October 2025

Keywords:
Enhanced oil recovery
Foam stability
Nanoparticles
Mobility reduction factor

A B S T R A C T

Oil reservoirs subjected to a gas recovery technique are commonly challenged by early gas breakthroughs affecting the production rate. Foam is injected to block and divert gas to reservoir sections, however, achieving this mechanism requires stable foam to withstand extreme reservoir conditions, such as temperature, pressure and salinity. In this work, synergy actions between amino-propyltriethoxysilane doped SiO_2 nanoparticles (NPs) and MFomax were investigated on rheology, interfacial tension (IFT), wettability, foam stability and quality to reduce gas mobility and enhance oil recovery (EOR). The formulation was guided by optimization, and the foam studies were carried out at optimum concentrations. Core-flood equipment was used to assess the gas mobility reduction factor (MRF) and EOR. From the findings, the foamability of the nanofluid is primarily governed by synergy action between the NPs and MFomax due to significant R^2 value (0.9; $p < 0.05$). Presence of NPs in the formulation resulted in good fluid properties such viscosity and IFT. The nanofoam stability has improved tremendously to 119% relative to MFomax foam. According to the IFT and contact angle, the detachment energy of the NPs (1.4×10^8 eV) is higher than 1 eV suggesting strong adsorption at aqueous interface leading to foam stability. The nanofoam reached a maximum of 50 MRF, while MFomax was below 40 MRF. Subsequently, all the foam descended to lower quality regions around 5 PVI due to the change in foam morphology. Furthermore, the EOR recorded by nanofoam demonstrates a 7% increase on top of MFomax recovery factor. Thus, it can be deduced that the synergy of SiO_2 NPs with MFomax offer several benefits in improving the foam stability, quality, MRF and EOR.

1. Introduction

Enhanced oil recovery (EOR) is a technology developed mainly to improve crude oil production (Barati-Harooni et al., 2019; Sivasankar and Kumar, 2019). The technique increased oil production rate to about 30–40 % on top of primary and secondary processes (15–30 %) (Takeya et al., 2019). The remaining 60 % of oil in the reservoir is scientifically believed to be withheld by micro and macroscopic factors such as interfacial tension (IFT), wettability, permeability (Emami Meybodi et al., 2011) and negative capillary force (Jing et al., 2019). The development of sweep-efficient fluids like foam is highly recommended to extract residual oil because of exponential global oil demand. Although, studies have reported that the sweep efficiencies of some fluids are affected by anisotropy or heterogeneity making the sweep conformance in reservoirs challenging (Hernando et al., 2018). However, the sweep efficiency can be enhanced by rising the

* Corresponding author. Institute of Hydrocarbon Recovery, Universiti Teknologi PETRONAS, 32610 Bandar Seri Iskandar, Perak Darul Ridzuan, Malaysia.
E-mail address: hamzafalal84@gmail.com (M.F. Hamza).

Peer review under the responsibility of Editorial Office of Petroleum Research.

https://doi.org/10.1016/j.ptlrs.2025.09.008

capillary number and enhancing the mobility ratio (Sivasankar and Kumar, 2019). The injection of water in alternation with gas (WAG) is the most extensively applied EOR technique (Afzali et al., 2018; Hamza et al., 2017a). Nevertheless, the challenge of high gas mobility in the WAG results in low oil sweeping because of early gas breakthrough (Farhadi et al., 2016). The use of surfactants has been envisioned as an efficient technique to prevent the gas from escaping. The water in the WAG can be substituted with a surfactant, and whenever gas is introduced, the formation of foam occurs. The foam is viewed as a gas bubble enclosed in aqueous liquid, preventing gas diffusion. The Snap-off mechanism due to gas movement via wet pores is the major leading mechanism of foam generation in the porous media (Hamza et al., 2017a). This process is called foam-assisted-water-alternating gas method (FAWAG) (Ahmadi et al., 2015). Nevertheless, the foam instability issues at higher temperatures are one of the major challenges with the FAWAG method, and this causes unexpected poor oil recovery (Yekeen et al., 2018). The bulk stability of the foam is measured by determining the half-life of the foam which is the time taken to attain half of the initial volume (Osei-Bonsu et al., 2017). In the bulk stability analysis, a longer half-life is a good sign of quality foams which determine the foam stability (Osei-Bonsu et al., 2015). In most cases, foam behavior at extreme conditions is investigated by using porous media and correlated with apparent viscosity (μ_{app}) to estimate foam characteristic (Tyrode et al., 2003). In addition, the quality of the foam can be assessed by mobility reduction factor (MRF) (Alcorn et al., 2017; Osei-Bonsu et al., 2016). The MRF is the ratio of pressure drop owing to the instantaneous gas injection into the porous body in the presence and absence of a surfactant (Rahmani, 2018). Foams with high MRF values are quality foams which have ability to spread consistently in the porous media (Hanamertani et al., 2018). Foams bubble size and their uniform distributions in aqueous phase are a characteristic feature of foam texture. Foam texture is a fundamental property essentially controlling the characteristic behavior of the MRF. In the porous medium, foams with good quality have population of smaller bubbles distributed evenly and are extremely resistant to flow than the bigger bubbles. The Weber Number (We) in Eq. (1) provides an expression used to characterize the foam texture which solely depends on shear stress (G), bubble radius (R) and IFT (γ) (DiCarlo et al., 2015).

$$We = \frac{G\mu sR}{\gamma} \tag{1}$$

The study of Memon et al. (2017) provides comparative studies on the MRF of different surfactant foams. The author significantly observed robust MRF values and attributed it to the synergy between surfactants. Although it there are limited studies to indicate a threshold of MFR value, however, Etminan et al. (2016) estimated that foam with a 50 % MRF could ensure high degree of gas mobility control.

Similarly, the foam μ_{app} can be calculated using Eq. (2) (Jones et al., 2016; Osei-Bonsu et al., 2016) which describes foam quality.

$$\mu app = \frac{k\nabla P}{(ul + ug)} \tag{2}$$

Where ∇P signifies the pressure gradient (Pa m^{-1}) across the core, k designates the permeability (m^2), u_l and u_g, respectively, are the liquid and gas superficial velocities (m s^{-1}).

Jones et al. (2016) explored different foam qualities by measuring the μ_{app} and established a plot relationship that explains two regions of foams' qualities. Furthermore, many studies have reported the effects of additives such as NPs, polymers, surfactants etc in enhancing rheology and foam stability (Hamza et al., 2018; Hernando et al., 2018; Ko and Huh, 2019; Vatanparast et al., 2017). The recent development of nanotechnology is gaining momentum because of their thermophysical properties, and a notable important benefit as foam stabilizers (Farhadi et al., 2016). Interestingly, NPs can be sourced from a variety of cost-effective materials such as clay, mineral rocks, and other materials (Paul et al., 2007) which are environmentally friendly. NPs have been investigated to improve the thermal properties and rheology of several foaming agents. For instance, Sun et al. (2014) used NPs to enhance foam's thermal and rheology properties. SiO_2 NPs is the most frequently used NPs owing to its availability, dispersibility, thermal resistance, and offers excellent IFT reduction in comparison to metal NPs (Worthen et al., 2013). It has the ability to adsorb at the interface and provide a barrier against foam rupture (Worthen et al., 2014; Xue et al., 2016). Many studies also reported that SiO_2 NPs increase hydrocarbon recovery when production ceases at secondary stage (Ahmadi and Shadizadeh, 2013). The surface of SiO_2 NPs is chemically modified to enhance its properties such as reaction side, size, interfacial and wetting behaviors. Detailed and extensive chemical modifications of the SiO_2 NPs with surfactants, coupling agents, or polymers have been reported (Park et al., 2010; Protsak et al., 2018; Wang et al., 2006; Xu et al., 2015).

The objective of this paper is to develop a nanofoam from combination of aminopropyltriethoxysilane functionalized SiO_2 NPs with MFomax surfactant to comprehensively investigate the foam properties, foamability, stability, quality, MRF and assess EOR.

2. Material and method

The aminopropyltriethoxy silane SiO_2 NPs with 20–30 nm diameter, bulk and true density of <0.10 and 2.4 g cm^{-3}, and surface area of 180–600 m^2 g^{-1} was supplied from the US Research Nanomaterials, Inc. USA. The MFomax surfactant, native reservoir sandstones and crude oil were supplied by PETRONAS Sdn Bhd, Malaysia.

2.1. Formulation

Synthetic brine (3.5 wt/v%) composed of NaCl, $MgCl_2.6H_2O$, $SrCl_2. 6H_2O$, Na_2SO_4, KCl, $NaHCO_3$, and $CaCl_2.2H_2O$ were prepared based on actual composition of Malaysia's oil reservoir. The brine was used in all the nanofluid preparations, and diluted to 1, 1.5, 2, 2.5 and 3 v/v% for subsequent analyses. In the preparation of the nanofluid (NF), Table 1 represents randomly designed experiments developed by Design Expert so that experimental bias in the form of error was minimized. The MFomax and SiO_2 NPs concentrations were kept within the range of 0.1–0.5%, respectively, for optimization. Each formulation was prepared in a 100 mL beaker and stirred using a magnetic stirrer for 12 h at 25 °C. To minimize the NPs agglomeration in the surfactant, the formulations were sonicated for 1 h at 25 Hz. Afterwards, the samples were aged for 2 weeks at 25 °C. Subsequently, to measure the chemical interaction between the SiO_2 NPs and the MFomax, the conductivity of the formulations was measured using a conductivity meter (Vernier Labquest 2). All preparations were subjected to initial foam screening for optimization.

2.2. Effect of temperature and salinity on viscosity

At the optimum condition, the NF comprising of 0.5 % SiO_2 and 0.4 % MFomax was prepared in different concentrations of brine (0, 1.5, 2, 2.5, 3 and 3.5 wt %) and subsequently measured their viscosities at 25 and 90 °C, respectively, using Antor paar modular compact rheometre (MCR 302).

Table 1
Randomized design of Nanofluid formulation at different concentrations.

Nanofluid	MFomax (%)	SiO_2 NPs (%)	Aging (days)
NF 13	0.3	0.3	3
NF 4	0.4	0.4	6
NF 2	0.4	0.2	6
NF 1	0.2	0.2	6
NF 3	0.2	0.4	6
NF 11	0.3	0.1	9
NF 16	0.3	0.3	9
NF 15	0.3	0.3	9
NF 9	0.1	0.3	9
NF 17	0.3	0.3	9
NF 18	0.3	0.3	9
NF 20	0.3	0.3	9
NF 19	0.3	0.3	9
NF 12	0.3	0.5	9
NF 10	0.5	0.3	9
NF 7	0.2	0.4	12
NF 8	0.4	0.4	12
NF 5	0.2	0.2	12
NF 6	0.4	0.2	12
NF 14	0.3	0.3	15

2.3. Interfacial tension and wettability studies

The IFT analysis was performed using an interfacial tension analyser (IFT 700) via a pendant drop method. The equipment was set at 90 °C and 2023 psi and subsequently the chamber was filled with brine and allowed undisturbed until both the temperature and pressure were normalized. Thereafter, an oil drop was carefully generated from the needle in the chamber until it was stable. A high-resolution camera captured the image automatically and transformed it to IFT value by DROP image advanced software based on Young-Laplace principles. After establishing the IFT of brine-oil phase (control), the same process was repeated for other fluids.

For wettability studies, the same equipment and operating conditions were used. The experiment began by filling the chamber with brine and an oil drop was created and stacked on the rock surface in the chamber. As soon as the oil drop was stable, the contact angle was immediately recorded. The same process was repeated for other fluids.

2.4. Foamability screening

According to the experimental days in Table 1, exactly 10 mL of each formulation was mechanically shaken consistently for 30 s to produce foam. The average foam heights were recorded. The analysis of variance (ANOVA) was applied to analyse the data for foamability.

2.5. Effect of temperature and salinity on foamability

At the optimum condition, exactly 30 ml of nanofluid and MFomax were formulated in series of brine with different concentrations (0, 1.5, 2, 2.5, 3 and 3.5 wt %). Another set of formulations were prepared in crude oil mixture (95:5 v/v % formulation: oil ratio). All the formulations were then heated at 90 °C and subsequently foams were immediately generated in 30 s using a laboratory blender. These experiments were conducted in replicates for mean foam volume. For foam stability at 90 °C, the foams were further subjected to heating in the oven to observe the stability with time.

2.6. Foam morphology studies: texture, bubble size and particle detachment energy

To study the foam distribution, bubble size, and coalescence process, the dynamic foam in the presence and absence of crude oil was analyzed using a microscopy (Olympus IX 53). The Weber Number (We), Eq. (1), was used to study the texture of the foam.

Since NPs adsorbs at the interface, the energy (E_d) required to remove from the interface depends on the IFT (γ) and contact angle (θ). Thus, it can be calculated using Eq. (3) (Farhadi et al., 2016).

$$E_d = \pi r^2 \gamma (1 \pm \cos\theta)^2 \tag{3}$$

Where, r is the foam bubble radius.

2.7. Multifluid HTHP coreflood: foam quality evaluation in porous media

Sanchez Technology V1.5740 (France) Multifluid HTHP core flood equipment was used for the purpose of this assessment. The equipment is ideal to simulate real reservoir conditions and has a capacity to withstand up to 10,000 psi and 200 °C. It is equipped with chambers of brine, oil, gas, and a chemical. A core holder is usually located in the compartment of the cell reinforced with injections and production valves where differential pressures (Δp) are detected. A summary of operation parameters used in the study has been presented in Table 2. Similarly, in the table, the properties of a native sandstone from Malaysia oil field have been described. Prior to mounting the sandstone in the core holder, adequate saturation with brine was performed using a high-pressure manual saturator for 24 h at a pressure of 1000 psi. To maintain the core saturation, the experiment started by injecting sufficient volume of brine at a constant flow rate of 0.2 cc min^{-1}. After that, approximately 1.5 PVI (pore volume of injections) of the nitrogen gas (N_2) was injected continuously at the same flow rate until no displacement of brine was observed. The change in pressure due to gas was observed as Δp-gas. Moreover, another circle of brine injection was repeated until the Δp was restored to its initial brine state, ensuring that all the gas had been removed. Subsequently, another PVI of the MFomax surfactant was injected at the same flow rate. To generate *in situ* foam, about 5 PVI of the N_2 gas was continuously injected into the MFomax saturated core and the Δp was observed to increase significantly indicating foam had been generated. The change in pressure was also recorded as Δp-foam due to the MFomax foam. The experiment due to the nanofluid was similarly conducted, and the Δp-nanofoam was likewise recorded.

All the data were analyzed and expressed into the foam quality known as the MRF using Eq. (4) (Abdelgawad et al., 2022).

$$Foam\ quality\ (MRF) = \frac{\Delta p\ foam}{\Delta p\ gas} \tag{4}$$

Table 2
Experimental conditions and physical properties of sampled reservoir sandstone.

Coreflood test parameters		Core properties	
Overburden pressure (Psi)	3023	Length (mm)	61.10
Injection pressure (psi)	2023	Diametre (mm)	37.50
Conc. of MFomax (v %)	0.4	Dry mass (g)	138.0
Conc SiO_2 NPs (wt %)	0.5	Sampling depth (ft)	6173
Brine (wt %)	3.5	Pore volume PV (cc)	15.60
Flow rate (cc min^{-1})	0.2	Porosity Ø (%)	23.10
Gas type	N_2	Permeability K_{air} (mD)	198.6
Test temperature (°C)	110		

2.8. Multifluid HTHP coreflood: foam EOR

Under the same conditions provided in Table 2 and using the same equipment, the oil displacement experiments of MFomax and nanofoam were studied. Initially the core was saturated with the brine for several PVI until the Δp was steady and recorded. After that, oil was then injected until no brine production was observed and oil production reached 100 %. To ensure sufficient oil saturation, the core was aged for two days at this stage. Subsequently, initial water saturation (*Swi*) and initial oil saturation (*Soi*) relative to the PVI and oil-in-place (*OIP*) were determined. Oil displacement by water flood (brine) was started by injecting several PVI of brine at 0.2 cc min^{-1} until no further oil production. Thus, oil recovery due to water flood relative to the OIP was computed. The residual oil after the water flood (Sor_w), i.e. oil in the interstitial pores of the rock that could not be recovered by water flood, was also determined.

To create a favourable environment for foam generation, several PVI of foaming agents (nano-fluid or MFomax) were injected. Immediately, the injection of N_2 gas was accompanied and foam was produced *in situ*. For foam generation, the flow rate of all injected fluids was likewise sustained at 0.2 cc min^{-1}. The oil recovery due to nano-foam and MFomax foam were recorded. After the experiment, the residual oil due to foam floodings were then determined.

3. Results and discussion

3.1. Chemical formulation

Conductivity is commonly used to assess the chemical interaction between binary mixtures. Presence of surface charges around the atoms or molecules may indicate high conductivity. Fig. 1 shows that SiO_2 NPs had the highest conductivity which is attributed to the modification with amino groups (Pan et al., 2016). MFomax, an amphoteric surfactant, exhibits lower conductivity than the SiO_2. Nevertheless, the conductivity in the case of a nanofluid mixture decreased after the formulation which indicates a good surface chemical interaction between the MFomax surfactant and NPs. The conductivity experiment is critical and is used to study adsorption of surfactants on NPs (Farhadi et al., 2016).

3.2. Statistical analysis of foamability

The ANOVA of the foamability is summarized in Table 3. The cubic model chosen demonstrates P < 0.05, indicating many model terms such as MFomax and NP were *significant,* describing their

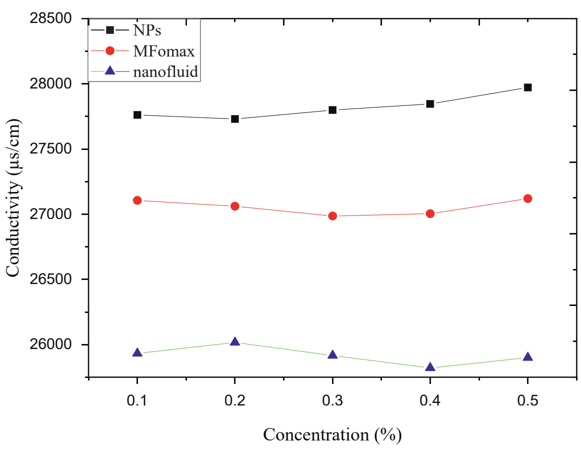

Fig. 1. Conductivity of the chemical formulation.

Table 3
The ANOVA of the foamability of the nano hybrid mixture (NF).

Model terms	Mean	SD	R^2	R^2 Adj.	R^2 Pred.	F value	P <0.05	
Cubic model	**102**	**4.95**	**0.9**	**0.8**	**0.7**	**11.8**	**0.0002**	***significant***
MFomax						6.1	0.0295	
SiO_2						31.1	0.0001	
MFomax* SiO_2						8.2	0.0145	
MFoamx*Aging						4.6	0.0535	
$MFomax^2$						15.1	0.0022	
$Aging^2$						6.4	0.0266	
MFoamx*SiO_2 *Aging						12.7	0.0039	
Lack of fit						0.5	0.7930	*not significant*

synergy action to influence foam volume. Furthermore, a high R square value supported by small differences between the adjusted and predicted R square indicates the good fitness of the data (Nguyen et al., 2014; Adamu et al., 2017). For any good model, a lack of fit test must be *not significant* so that all model terms can have effects on the foamability. The optimum concentrations of the MFomax and SiO_2 NPs were 0.4 % and 0.5 %, respectively. These optimum conditions were used for all the subsequent investigations.

3.3. Effects of salinity and temperature on viscosity

From Fig. 2a and b, there were direct relationships between the viscosity and salinity concentrations at both 25 and 90 °C, respectively. Meaning that, viscosity increases with salinity. This

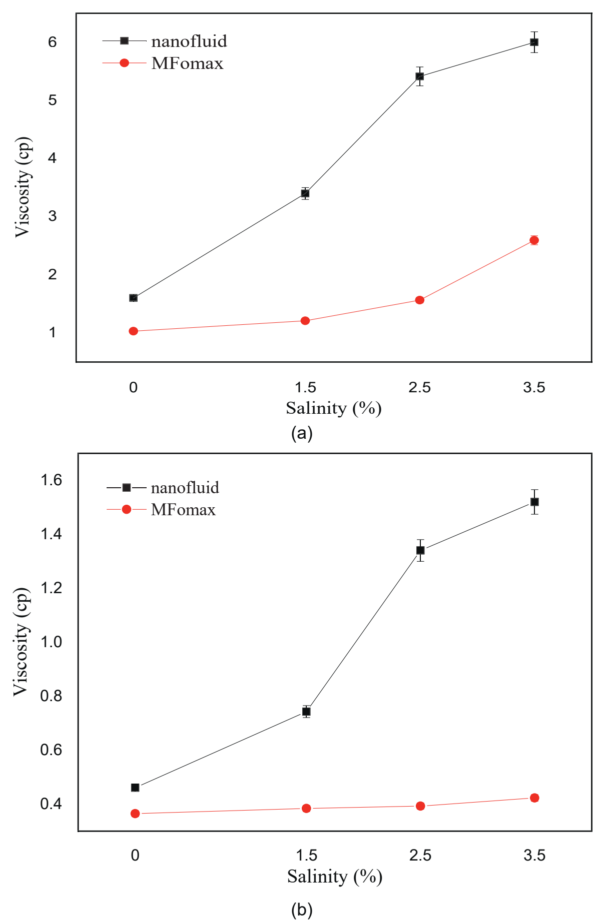

Fig. 2. Salinity and temperature effect at (a) 25 °C and (b) 90 °C on the viscosity of the formulation.

observation may suggest transformations of micelle shapes from spherical to cylindrical (Kamranfar and Jamialahmadi, 2014). The cylindrical shape is inflexible which causes a rise in viscosity. Furthermore, at 90 °C, there was a substantial decrease in the viscosities of the MFomax and nanofluid having their viscosities less than 1.6 cp. High temperature is a critical factor that affects the viscosity and eventually reduces foam stability (Hamza et al., 2017b). A good formulation should withstand temperature change reasonably to enable the formation of quality foam in porous bodies (Osei-Bonsu et al., 2015). Remarkably, the presence of the SiO_2 NPs in the nanofluid (Fig. 2b) plays a pivotal role in ensuring good viscosities at different brine concentrations. For example, at extreme conditions, 3.5 % and 90 °C, the viscosity of nanofluid is 1.097 cp higher than the MFomax.

3.4. Interfacial tension, contact angle and detachment energy

Table 4 summarizes the IFT (γ) analysis of the brine, MFomax and nanofluid. The results show that the IFT of the base case system i.e. crude oil/brine was found to be 8.61 ± 0.4 mN/m. This represented the existing IFT in the sandstone reservoir. However, after adding 0.4 v % MFomax surfactant in the crude/brine system, a 73 % reduction of IFT was achieved. The reduction in IFT value is one of the major advantages of surfactants which can facilitate the release of crude oil from the rock (Luo et al., 2018). Moreover, a further reduction of the IFT value by 83% was significantly observed when MFomax was treated with 0.5 wt % SiO_2 NPs at the same concentration. The synergy between SiO_2 NPs and MFomax promotes additional surface activity better than the pure MFomax. SiO_2 NPs has been reported to demonstrate similar micelle rearrangement (Worthen et al., 2013).

Similarly, in Table 4, when the contact angle was studied, the system in brine saturation displayed water-wet ($\theta < 90°$) behavior. In water-wet systems, the sandstones have more affinity to retain water in exchange for oil which can make the oil easily accessible and extractable. Interestingly, both the injection of MFomax and nanofluid did not alter the wetting behaviors of the sandstones because the contact angles were all below 90°. A change in θ from 49 to 79° could be ascribed to the effect of the silane coating agent on the surface of SiO_2 NPs (Huaiyuan et al., 2009).

According to the IFT and θ results, the E_d was computed to be 2.7 x10^{-11} J which is equal to 1.4×10^8 eV higher than 1 eV (1.6 x 10^{-19} J), this suggests a huge detachment energy. This theory indicates that SiO_2 NPs can adsorb strongly and irreversibly at the interface of the foam and offer strong stability on the foam (Ko and Huh, 2019). This hypothesis was supported by Farhadi et al. (2016) where the authors report that for θ close to 90°, the NPs can stabilize the foams and have higher adhesion energy, while for $\theta < 30°$ or $\theta > 150°$, the NPs cannot stabilize foams and E_d would be low. In this regard, presence of NPs in MFomax increased the θ value towards 90°, signifying adsorption at interface. According to Dadi and Maurya (2025), nanoparticle with approximately 10 nm size having θ with a near 90°, the Ed can be above 1000 KT (25.68 eV). The high detachment energy of nanoparticles ensures irreversible adsorption at the gas–liquid interface, increasing the membrane strength, enhances the elasticity, and minimizes the diffusion of gas between neighboring bubbles. Furthermore, the drainage of the foam may eventually be reduced, and the foam remains stable for a longer time. One of the variables influencing the detachment energy and the maximum capillary force is the contact angle, as shown by the formulas for detachment energy and maximum capillary force. As the contact angle θ decreases, the particles' detachment energy decreases, and as the contact angle θ decreases, the maximum capillary force increases. To choose the nanoparticles with the optimal contact angle, it is therefore essential to thoroughly consider the detachment energy and the maximal capillary force (Sun et al., 2024). Rahim Risal et al. (2018) have demonstrated that some hydrophobic silica nanoparticles generate a larger detachment energy, which successfully stabilizes the carbon dioxide foam interface by irreversible attachment, making the foam layer thicker and improving the foam membrane's interfacial flexibility.

Table 4
The IFT and contact angle measurements.

Formulation of solution	γ (mN/m)	θ (°)
Brine (3.5 wt %)	8.61 ± 0.4	49 ± 1.7
MFomax (0.4 v %)	2.33 ± 1.8	63 ± 1.2
Nanofluid (0.4 v % MFomax + 0.5 wt % SiO_2 NPs)	0.39 ± 0.2	79 ± 7.5

3.5. Effect of salinity and temperature on the foamability

Fig. 3a presents the effects of the salinity in the absence and presence of crude oil at 90 °C on the foamability. As can be observed, the foams produced in the absence of salt had the highest foam volumes in comparison to their respective foam volumes in the presence of salt. This is because the salts ions limit the diffusion movement of surfactant molecules to the interface of air-water (Behera et al., 2014). Additionally, at this free salt condition, MFomax foam recorded higher foam volumes than the

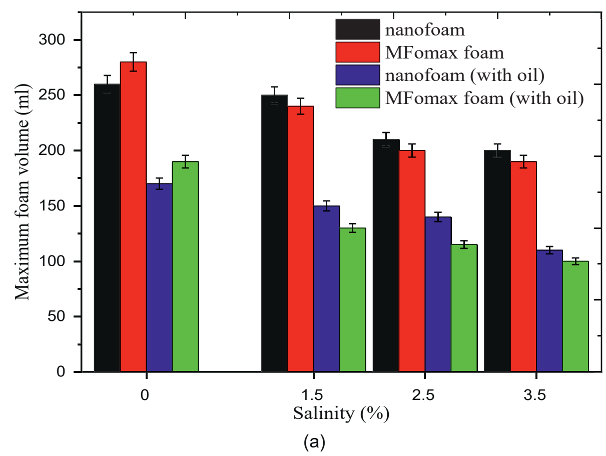

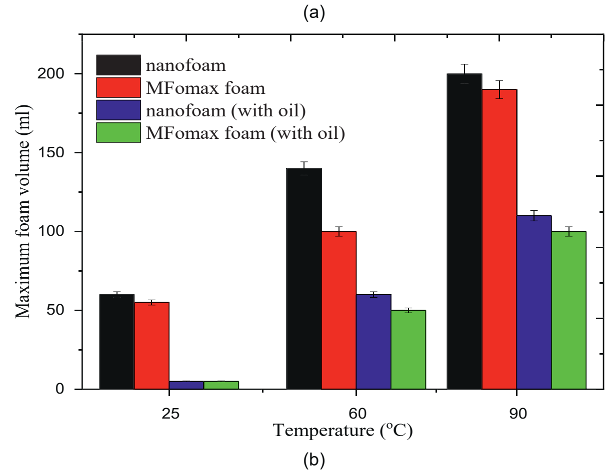

Fig. 3. (a) Effect of salinity on the foamability in the present and absence of crude oil at 90 °C (b) Effect of temperature on the foamability in the presence and absence of crude oil at 3.5 % salinity.

nanofoam. However, by increasing the salt concentration, it resulted in the decreasing of foam volumes affecting both the MFomax and nanofoam. Interestingly, the nanofoam demonstrated salt tolerance more than the MFomax foams, which was due to the presence of SiO_2 NPs (Negin et al., 2016; Zhu et al., 2014). Other than the effect of salinity, the presence of crude oil further affects the foamability of all kinds of foams. Factors such as oil entering and spreading in the aqueous film, and rate of film thinning are mechanisms attributed to the reduction of foam volume (Belhaij et al., 2014; Sun et al., 2018). However, the presence of SiO_2 NPs in the nanofoam provides a barrier against foam rupture.

The foam volumes under the worst-case salinity (3.5 %) were further investigated at ambient and higher temperature. Fig. 3b shows that at 25 °C both the MFomax and nanofoam produced low foam volumes in the presence and absence of crude oil. At ambient temperatures, high viscosity is preferred so that when fluid is subjected to higher reservoir temperatures it is likely to experience small effect, thus, ensuring quality foams (Wu and Pan, 2010). It was further observed that, with an increase in temperature from 25 to 90 °C, there was a substantial foamability improvement. The improvement in foamability was owing to the complex salt decomposition in accordance with the chemistry of water hardness. Wei et al. (2017), in his investigation observed similar behaviour. The foamability of MFomax and nanofluid in the presence of oil were also improved at 90 °C. Details information of crude oil effects on foam has been reported (Talebian et al., 2015).

3.6. Foam stability

The relative foam height, which is the ratio of average foam height to the initial foam height was used in this study to observe the foam rupture/decay behavior (Fig. 4). It can be observed that crude oil foams decompose faster than the crude oil-free foams. This is commonly caused by the entering and spreading of crude oil into the foam which results in the rapid foam collapse (Belhaij et al., 2014). The rapid foams deterioration from initial volume to 5 min was influenced by the draining of the liquid from the bulk foam (Hanamertani et al., 2018). Subsequently, the foams remained stable for some time with substantial enhancements notably in the case of the nanofoam owing to the SiO_2 NPs than the MFomax.

The results of salinity effects on foam rupture behaviors are shown in Fig. 5. It was observed that at free brine condition in Fig. 5a, there was rapid foams decay. Approximately, 20 and 13 % of the MFomax and nanofoam decomposed in free brine regions, respectively. Nevertheless, at 1.5 wt % salinity (Fig. 5b), there were improvements of foams rupture up to 25 and 30 min in each case owing to the interaction of the foams with the salt ions. Thereafter, an increase in brine concentrations to 2.5 and 3.5 % (Fig. 5c and d) triggered more rapid decay in the case of MFomax foam than the nanofoam, describing that MFomax could no longer resist high salt concentrations.

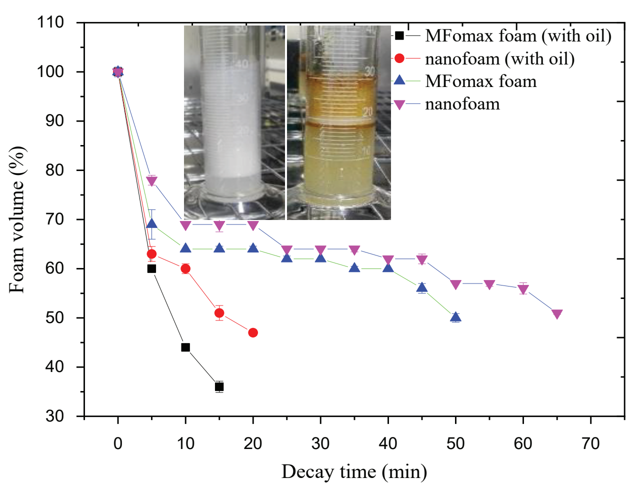

Fig. 4. Effect of crude oil on the foam decay profile at 90 °C.

Fig. 6 displays the foam half-lives results. Generally, crude oil foams had shorter half-lives than the foams in the absence of crude oil for both MFomax and nanofoam, respectively, describing that the presence of crude oil has unfavourable effects on the foam stability. However, the MFomax foam stability was reduced by 85 % owing to the crude oil effect than the nanofoam (75 %). Furthermore, in the absence of crude oil, the interaction between the MFomax and the SiO_2 NPs in the nanofoam enhanced the foam's thermal stability by 30 % in relation to the MFomax foam. However, the interaction was found to be more effective in the crude oil. The enhancement in this condition was found to be higher than the MFomax foam by a factor of 119 %. NPs have been reported to separate foam bubbles against coalescence, thus ensuring longer stability (Nazari et al., 2017).

Fig. 6b shows the effect of salinity results on foam stability at 90 °C. In the absence of brine (0 wt/v %) brine, the nanofoam was more stable than MFomax foam which could be attributed to the presence of SiO_2 NPs. The stability was improved by 125 % relative to the MFomax foam stability. However, by increasing brine concentration to 1.5 %, had caused the foam stability of both MFomax and nanofoam to also increase. It was ascertained by the interaction between the salt ions and surfactant charges leading to increase in foam stabilities. Studies reported in (Kalyanaraman et al., 2015) highlights this phenomenon and observed an increase in foam stability at low brine concentration. Moreover, further increase in the concentration of brine to 2.5 and 3.5 %, a decrease in the stability of the foam was observed in both MFomax and the nanofoam. This indicates that foams had the best stabilities in the 1.5 wt % brine concentration than in absence or higher salt concentration. This is a similar behavior to the aforementioned decay profile. Nevertheless, since reservoirs are associated with high salinity, our result indicated that at extreme salinity of 3.5 %, the nanofoam stability improved by 119 % higher than its precursor MFomax foam.

3.7. Foam morphology: bubble size, texture and rupture behavior

The foams morphology with respect to the decay profile were visually investigated using a high-resolution microscope. Each MFomax foam and nanofoam were charaterized in the absence and presence of brine, as well as in crude oil. The foams micrographs have been presented in Fig. 7. All the foam structures at the initial time appeared slightly circular bubbles. But as the time progresses the bubbles' structures transformed to polyhedron shape due to minimum energy principles that relate liquid volume fraction (ϕ) and time. If $\phi > 0.15$, the foam is described as a “wet foam” and its bubble shape appear as circular. However, when $\phi < 0.05$, the bubble shape becomes polyhedrons, and this state is described as a “dry foam” (Furuta et al., 2016). Similarly, in the absence and presence of brine the nanofoam was observed with more population of small bubbles dominating the continuous phase at initial time. After 60 min, the sizes enlarged, signifying foam coalescence had occurred. This is likewise in the presence of oil. By using the optical instrument, the foam bubbles were quantified to observe the range of size distributions in different conditions summarized in Table 5.

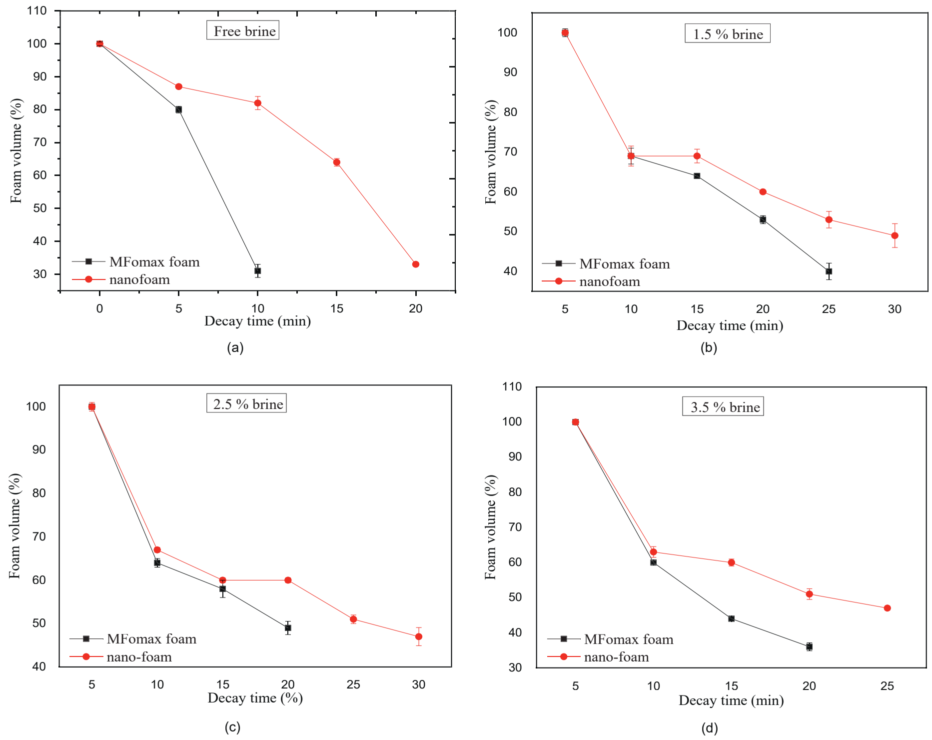

Fig. 5. Effect of salinity on the foam decay profile at 90 °C.

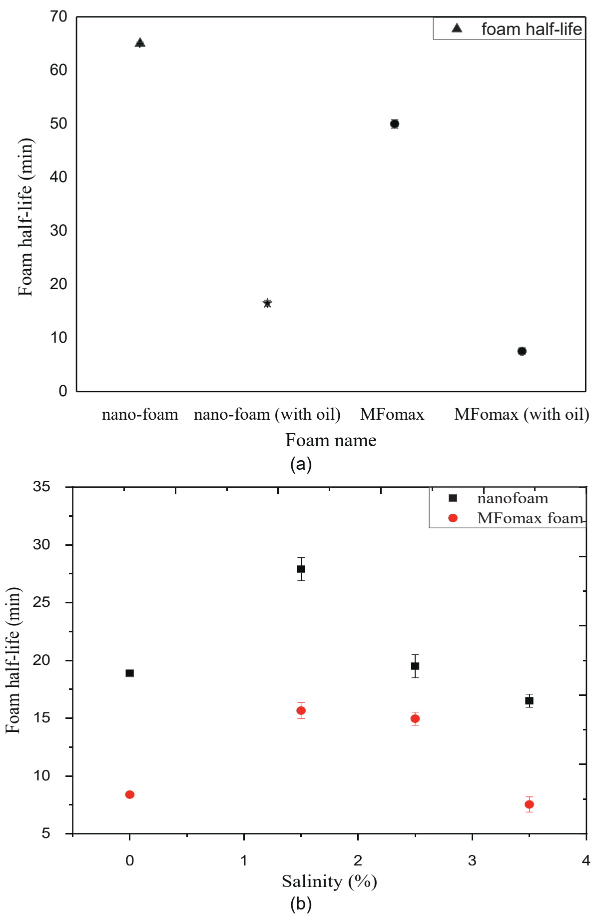

Fig. 6. (a) Effect of temperature (90 °C) on foam stability in the absence and presence of crude oil. (b) Effect of salinity on foam stability at 90 °C in the presence of crude oil.

Furthermore, the average foam bubbles were plotted as a function of time in Fig. 8. Observations indicated that foam sizes in free brine, brine and crude oil for MFomax and nanofoam increase with time. Coalescence process results in an increase in bubble size due to fusing of smaller bubbles and eventually leads to foam rupture (Bisperink et al., 1992). Thickness of foam lamella and plateau region of small bubbles ensures foam's safety and enhances stability than the bigger bubbles. The nanofoam in brine was observed to have smaller bubble sizes than the MFomax foam in brine. Likewise, when nanofoam was produced in the presence of oil and brine. The presence of NPs and dissolved ions prevents or minimizes coalescence and eventually improves foam's life span.

The texture of the foam was determined using the We expression in Eq. (1) which depends on bubble radius (R), IFT, and the shear stress. The lower IFT of the nanofluid system resulted in a larger We which describes finer foam texture (smaller bubbles) (Worthen et al., 2013). Based on the We, the presence of the SiO_2 NPs in the nanofoam increased the foam texture by a factor of 12 times more than the MFomax foam. This was attributed to the influence of SiO_2 NPs on MFomax to improve viscosity and IFT.

3.8. Foam quality assessment in porous media

The foams quality was studied in the porous media to reflect the reservoir conditions. The MRF was used to evaluate the foam quality by determining the ratio of the Δp in the presence and absence of foam in porous media. Fig. 9 shows that when foams propagate in the sandstone, they demonstrate good qualities up to 2 PVI regions due to high MRF observed. In this region both the foams had their best qualities. The nanofoam reached a maximum of 50 MRF, while MFomax was below 40 MRF. Subsequently, all the foam descended to lower quality regions up to 5.5 PVI due to foam becoming drier (Hanamertani et al., 2018). Consequently, the nanofoam achieved about 55 % quality enhancement more than

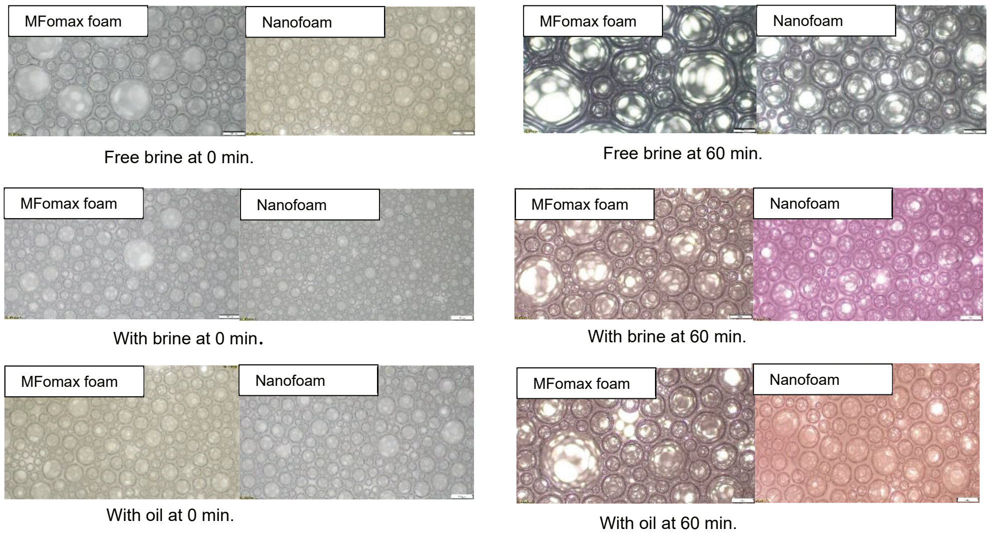

Fig. 7. Distribution and bubble size of the foam in the presence and absence of crude oil and salinity.

Table 5
Foam bubble size distribution in different regimes.

Time	Free brine foam		Brine foam		Brine + Crude oil foam	
	MFomax (μm)	Nano-foam (μm)	MFomax (μm)	Nano-foam (μm)	MFomax (μm)	Nano-foam (μm)
0	83–1016	42–654	91–843	32–288	63–563	93–545
30	127–1515	56–1057	89–963	40–640	75–1245	60–663
60	125–1638	97–827	120–1164	75–687	114–1577	131–825

the MFomax foam which signifies foam's strength and good quality (Memon et al., 2017).

3.9. Foam EOR

The oil recovery due to water flood was about 30–31 % after injecting 1.6 PVI brine. Water breakthroughs were observed around 0.3 PVI for all the two cases. After the water flood, the residual oil (Sor_w) was calculated to be about 49–52 % in the sandstone pores. The Sor_w trapped oil in sandstone arises due to several phenomena such as viscous or capillary force (Suthar et al., 2008). Accordingly, the injection of the foam was used as a tertiary or an EOR technique to maximize oil production. After injecting 5.5 PVI foams, both the MFomax and nanofoam foam showed notable EOR before the gas breakthrough were observed at 2.8 and 3.0 PVI, respectively. Foam can avert gas to various sections in the porous media which can lead to significant EOR (Shabib-asl et al., 2014). The recovery factor with nanofoam was found to be 26.29 % which was higher than the MFomax foam (19.08 %). This improvement could be attributed to several factors demonstrated by nanofluid in the aforementioned sections such as presence of NPs, good viscosity, IFT, foam bubble size, foam stability and foam quality (MRF). Therefore, the cumulative EOR was found to be 48.83 % for MFomax and 56.48 % for nanofoam.

In summary, the key findings of this study aligned with various important parameters in Table 6. The data in the table provides comparative insight of this study with previous literature.

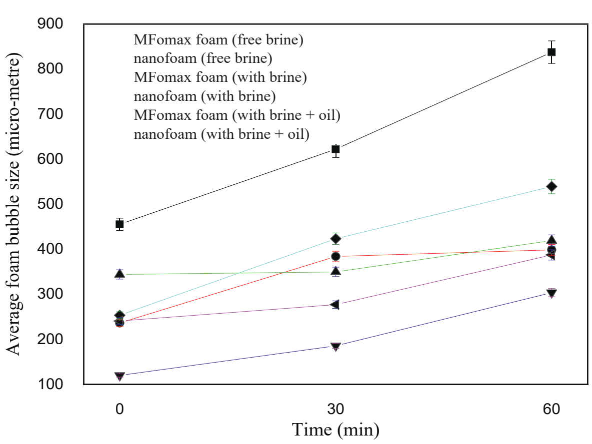

Fig. 8. Average foam bubble size in the presence and absence of crude oil and salinity.

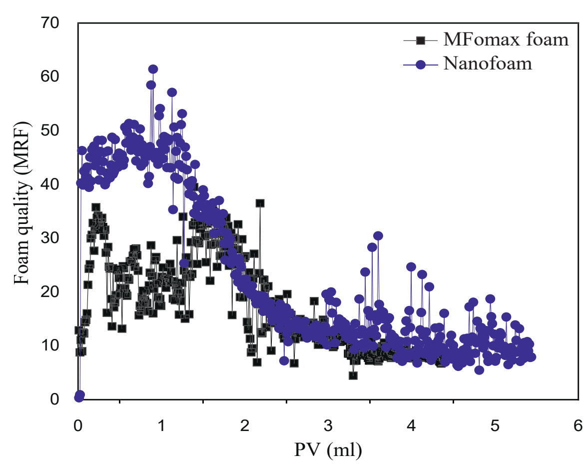

Fig. 9. Evaluation of foam quality at 110 °C and 2023 psi in the porous media.

Table 6
Insights into the roles of different NPs and their synergy with surfactants on various EOR parameters.

References	Composite Nanofluid		Foam stability (min.)	Bubble Size (μm)	Ed (eV)	IFT (mN/m^2)	ϑ (o)	MRF	EOR (%)
	NPs	surfactant							
This study	Coated SiO_2	MFomax	65	250–310	1.4 x 10^8 Reports principles	0.39	79	50	56.5
Ahmadi (2023)	CaO	–	–	–	–	–	–	–	73
Ahmadi et al. (2024)	Coated ZnO/SiO_2	–	–	–	–		74	–	52
Dadi and Maurya (2025)	SiO_2	SDS	56	–	Reports principles	–	–	–	–
Joshi et al. (2025)	$CaCO_3$	AOS	55	50	Report principles	1.68	–	–	65
Joshi et al. (2025)	BN	AOS	47	–	Report principles	–	–	–	–
Dadi and Maurya (2025)	Al_2O_3	AOS	93	371	Report principles	6.91	–	4.5	–
Ilkhani et al. (2022)	TiO_2	SDS	12.2	133	Report principles	4.3	128	–	81
Ilkhani et al. (2022)	ZnO	SDS	7.5	201		4.4	130	–	78
Dadi and Maurya (2025)	SiO_2	DATB	45	–	Report principles	–	–	–	–
Dadi and Maurya (2025)	Al_2O_3	CAPB	138	280	Report principles	4.5	–	–	–
Dadi and Maurya (2025)	SiO_2	AOS	76	394	Report principles	–	–	–	–
Dadi and Maurya (2025)	Al_2O_3	SDS	58	–	Report principles	–	–	–	–
Dadi and Maurya (2025)	SiO_2	CTAB	53	426	Report principles	4.23	–	–	–
Dadi and Maurya (2025)	Al_2O_3	CTAB	39	472	Report principles	–	–	–	–
Dadi and Maurya (2025)	Al_2O_3	DTAB	36	–	Report principles	–	–	–	–
Dadi and Maurya (2025)	SiO2	CAPB	115	310	Report principles	–	–	–	–

4. Challenges and limitations

NPs have significant potential in revolutionizing oil and gas sectors, and present successes in laboratory scales. However, cost and mechanism of NPs synthesis, anticipation of aggregation and effective transport through porous rock in reservoir conditions are the main scalability issues when employing NPs for real field applications (Iravani et al., 2023; Zhou et al., 2023). The need to develop promising methods for large-scale production and eco-friendliness is crucial. This may involve exploring principles of green chemistry techniques such as atom economy, design safer chemicals, use of renewable feedstocks, reducing derivatives, real-time pollution analysis and optimizing existing chemical synthesis processes (Duan et al., 2015; Iravani et al., 2023). Incorporating viscoelastic polymers into nanofluid can prolong foam resistance to deformation, ensuring quality and promoting stability (Li et al., 2025). Venturing into more research and development in addressing these challenges is crucial to avail the opportunities of nanotechnology which eventually can become a more viable and impactful tool for EOR.

5. Conclusion

A comprehensive experiment has been conducted aimed at investigating the influence of coated SiO_2 NPs on the performance of MFomax surfactant and its foam. The foamability of the nanofluid is primarily governed by synergy action between the MFomax and NPs with significant R^2 value (0.9). Presence of NPs in the formulation resulted in improved fluid properties such viscosity and IFT. The foam generated from the nanofluid has been dominated by smaller bubble sizes and demonstrates good quality and stability according to the assessment of MRF. The MRF of the nanofoam reached a maximum value of 50 in comparison with an MRF of below 40 achieved by MFomax without NPs. The recovery factor with nanofoam was found to be 26.29 % which was higher than the MFomax foam (19.08 %). These findings demonstrate that coated SiO_2 NPs combined with MFomax has the potential to revolutionize oil reservoirs when deployed in foam flooding techniques.

CRediT authorship contribution statement

Mohammed Falalu Hamza: Writing – original draft, Methodology, Investigation, Formal analysis, Conceptualization. **Hassan Soleimani:** Writing – review & editing, Supervision, Project administration, Funding acquisition. **Bashir Abubakar Abdulkadir:** Writing – review & editing. **Saifullahi Shehu Imam:** Writing – review & editing. **Sabiha Hanim Saleh:** Writing – review & editing. **Yarima Mudassir Hassan:** Writing – review & editing.

Declaration of competing interest

The authors declare that they have no known competing financial interests or personal relationships that could have appeared to influence the work reported in this paper.

Acknowledgement

The authors of this paper have appreciated the support of the project (Grant: PRSB EPTD 513CB010) from the PETRONAS Research Sdn, Bhd,. The authors express acknowledgement to the Institute of Hydrocarbon Recovery, Universiti Teknologi Petronas, Malaysia, Bayero University Kano, Nigeria, and Universiti Teknologi Mara, Malaysia.

References

Abdelgawad, K.Z., Adebayo, A.R., Isah, A., Muhammed, N.S., 2022. A literature review of strength and stability of foam and their relationship with the absolute permeability of porous media. J. Petrol. Sci. Eng. 211, 110195.
Adamu, M., Mohammed, B.S., Shafiq, N., 2017. Flexural performance of nano silica modified roller compacted rubbercrete. Int. J. Adv. Appl. Sci. 4 (9), 6–18.
Afzali, S., Rezaei, N., Zendehboudi, S., 2018. A comprehensive review on enhanced oil recovery by water alternating gas (WAG) injection. Fuel 227, 218–246.
Ahmadi, M.A., Shadizadeh, S.R., 2013. Induced effect of adding nano silica on adsorption of a natural surfactant onto sandstone rock: experimental and theoretical study. J. Petrol. Sci. Eng. 112, 239–247.
Ahmadi, Y., 2023. Improving fluid flow through low permeability reservoir in the presence of nanoparticles: an experimental core fooding WAG tests. Iranian J. Oil Gas Sci. Tech. 12 (2).
Ahmadi, Y., Eshraghi, S.E., Bahrami, P., Hasanbeygi, M., Kazemzadeh, Y., Vahedian, A., 2015. Comprehensive Water–Alternating-Gas (WAG) injection study to evaluate the most effective method based on heavy oil recovery and asphaltene precipitation tests. J. Petrol. Sci. Eng. 133, 123–129.
Ahmadi, Y., Malekpour, M., Kikhavani, T., Bayati, B., 2024. The study of the spontaneous oil imbibition in the presence of new polymer-coated nanocomposites compatible with reservoir conditions. Petrol. Sci. Tech. 42 (8), 974–992.
Alcorn, Z.P., Fredriksen, S.B., Sharma, M., Fernø, M.A., Graue, A., 2017. CO_2 foam EOR field pilot-pilot design, geologic and reservoir modeling, and laboratory investigations. In: IOR 2017-19th European Symposium on Improved Oil Recovery.
Barati-Harooni, A., Najafi-Marghmaleki, A., Hoseinpour, S.A., Tatar, A., Karkevandi-Talkhooncheh, A., Hemmati-Sarapardeh, A., Mohammadi, A.H., 2019. Estimation of minimum miscibility pressure (MMP) in enhanced oil recovery (EOR) process by N_2 flooding using different computational schemes. Fuel 235, 1455–1474.

Behera, M.R., Varade, S.R., Ghosh, P., Paul, P., Negi, A.S., 2014. Foaming in micellar solutions: effects of surfactant, salt, and oil concentrations. Ind. Eng. Chem. Res. 53 (48), 18497–18507.

Belhaij, A., AlQuraishi, A., Al-Mahdy, O., 2014. Foamability and foam stability of several surfactants solutions: the role of screening and flooding. In: SPE Kingdom of Saudi Arabia Annual Technical Symposium and Exhibition.

Bisperink, C.G.J., Ronteltap, A.D., Prins, A., 1992. Bubble-size distributions in foams. Adv. Coll. Interf. Sci. 38, 13–32.

Dadi, N.R., Maurya, N.K., 2025. Keys to enhancing efficiency in nanoparticle-based foam EOR: experimental insights into different types of surfactant-nanoparticle interactions. J. Mol. Liq. 422, 126927.

DiCarlo, D., Huh, C., Johnston, K.P., 2015. Area 2. Use of Engineered Nanoparticle-Stabilized CO_2 Foams to Improve Volumetric Sweep of CO_2 EOR Processes. Univ. of Texas, Austin, TX (United States).

Duan, H., Wang, D., Li, Y., 2015. Green chemistry for nanoparticle synthesis. Chem. Soc. Rev. 44 (16), 5778–5792.

Emami Meybodi, H., Kharrat, R., Wang, X., 2011. Study of microscopic and macroscopic displacement behaviors of polymer solution in water-wet and oil-wet media. Transp. Porous Med. 89 (1), 97–120.

Etminan, S.R., Goldman, J., Wassmuth, F., 2016. Determination of optimal conditions for addition of foam to steam for conformance control. In: SPE EOR Conference at Oil and Gas West Asia.

Farhadi, H., Riahi, S., Ayatollahi, S., Ahmadi, H., 2016. Experimental study of nanoparticle-surfactant-stabilized CO_2 foam: stability and mobility control. Chem. Eng. Res. Des. 111, 449–460.

Furuta, Y., Oikawa, N., Kurita, R., 2016. Close relationship between a dry-wet transition and a bubble rearrangement in two-dimensional foam. Sci. Rep. 6 (1), 37506.

Hamza, M.F., Sinnathambi, C.M., Merican, Z.M.A., Soleimani, H., Karl, S.D., 2017a. An overview of the present stability and performance of EOR-foam. Sains Malays. 46 (9), 1641–1650.

Hamza, M.F., Sinnathambi, C.M., Merican, Z.M.A., 2017b. Recent advancement of hybrid materials used in chemical enhanced oil recovery (CEOR): a review. In: IOP Conference Series: Materials Science and Engineering.

Hamza, M., Sinnathambi, C., Merican, Z., Soleimani, H., Stephen, K.D., 2018. Effect of SiO_2 on the foamability, thermal stability and interfacial tension of a novel nano-fluid hybrid surfactant. Int. J. Adv. Appl. Sci. 5 (1), 113–122.

Hanamertani, A.S., Pilus, R.M., Manan, N.A., Mutalib, M.I.A., 2018. The use of ionic liquids as additive to stabilize surfactant foam for mobility control application. J. Petrol. Sci. Eng. 167, 192–201.

Hernando, L., Satken, B., Omari, A., Bertin, H., 2018. Transport of polymer stabilized foams in porous media: associative polymer versus PAM. J. Petrol. Sci. Eng. 169, 602–609.

Huaiyuan, W., Xin, F., Yijun, S., Xiaohua, L., 2009. A study on the tribological properties of self-assembled method treated nano-La 2O3 filled PTFE/PEEK composites. J. Reinf. Plast. Comp. 28 (6), 645–655.

Ilkhani, M., Bayat, A.E., Harati, S., 2022. Applicability of methane foam stabilized via nanoparticles for enhanced oil recovery from carbonate porous media at various temperatures. J. Mol. Liq. 367, 120576.

Iravani, M., Khalilnezhad, Z., Khalilnezhad, A., 2023. A review on application of nanoparticles for EOR purposes: history and current challenges. J. Pet. Explor. Prod. Technol. 13 (4), 959–994.

Jing, W., Huiqing, L., Genbao, Q., Yongcan, P., Yang, G., 2019. Investigations on spontaneous imbibition and the influencing factors in tight oil reservoirs. Fuel 236, 755–768.

Jones, S.A., Van Der Bent, V., Farajzadeh, R., Rossen, W.R., Vincent-Bonnieu, S., 2016. Surfactant screening for foam EOR: correlation between bulk and core-flood experiments. Colloids Surf. A Physicochem. Eng. Asp. 500, 166–176.

Joshi, D., Ramesh, D.N., Prakash, S., Saw, R.K., Maurya, N.K., Rathi, K.B., Mitra, S., Sinha, O.P., Bikkina, P.K., Mandal, A., 2025. Formulation and characterisation of polymer and nanoparticle-stabilized anionic surfactant foam for application in enhanced oil recovery. Surf. Interfaces 56, 105615.

Kalyanaraman, N., Arnold, C., Gupta, A., Tsau, J.S., Barati, R., 2015. Stability improvement of CO_2 foam for enhanced oil recovery applications using polyelectrolytes and polyelectrolyte complex nanoparticles. In: SPE Asia Pacific Enhanced Oil Recovery Conference.

Kamranfar, P., Jamialahmadi, M., 2014. Effect of surfactant micelle shape transition on the microemulsion viscosity and its application in enhanced oil recovery processes. J. Mol. Liq. 198, 286–291.

Ko, S., Huh, C., 2019. Use of nanoparticles for oil production applications. J. Petrol. Sci. Eng. 172, 97–114.

Li, J., Xu, B., Zhu, L., He, X., Yang, J., Li, Y., Liu, T., 2025. Mechanism of polymer regulated high internal phase CO_2-in-water foam viscoelasticity for enhanced oil recovery. Fuel 384, 134050.

Luo, H., Zhang, Y., Fan, W., Nan, G., Li, Z., 2018. Effects of the non-ionic surfactant (CiPOj) on the interfacial tension behavior between CO_2 and crude oil. Energy & Fuels 32 (6), 6708–6712.

Memon, M.K., Shuker, M.T., Elraies, K.A., 2017. Study of blended surfactants to generate stable foam in presence of crude oil for gas mobility control. J. Pet. Explor. Prod. Technol. 7 (1), 77–85.

Nazari, N., Tsau, J.S., Barati, R., 2017. CO_2 foam stability improvement using polyelectrolyte complex nanoparticles prepared in produced water. Energies 10 (4), 516.

Negin, C., Ali, S., Xie, Q., 2016. Application of nanotechnology for enhancing oil recovery–A review. Petrol. 2 (4), 324–333.

Nguyen, X.H., Bae, W., Gunadi, T., Park, Y., 2014. Using response surface design for optimizing operating conditions in recovering heavy oil process, peace river oil sands. J. Petrol. Sci. Eng. 117, 37–45.

Osei-Bonsu, K., Grassia, P., Shokri, N., 2017. Relationship between bulk foam stability, surfactant formulation and oil displacement efficiency in porous media. Fuel 203, 403–410.

Osei-Bonsu, K., Shokri, N., Grassia, P., 2015. Foam stability in the presence and absence of hydrocarbons: from bubble-to bulk-scale. Colloids Surf. A Physicochem. Eng. Asp. 481, 514–526.

Osei-Bonsu, K., Shokri, N., Grassia, P., 2016. Fundamental investigation of foam flow in a liquid-filled Hele-Shaw cell. J. Coll. Interf. Sci. 462, 288–296.

Pan, H., Lu, Y., Song, L., Zhang, X., Hu, Y., 2016. Fabrication of binary hybrid-filled layer-by-layer coatings on flexible polyurethane foams and studies on their flame-retardant and thermal properties. RSC Adv. 6 (82), 78286–78295.

Park, J.T., Seo, J.A., Ahn, S.H., Kim, J.H., Kang, S.W., 2010. Surface modification of silica nanoparticles with hydrophilic polymers. J. Ind. Eng. Chem. 16 (4), 517–522.

Paul, K.T., Satpathy, S.K., Manna, I., Chakraborty, K.K., Nando, G.B., 2007. Preparation and characterization of nano structured materials from fly ash: a waste from thermal power stations, by high energy ball milling. Nanoscale Res. Lett. 2 (8), 397.

Protsak, I., Pakhlov, E., Tertykh, V., Le, Z.C., Dong, W., 2018. A new route for preparation of hydrophobic silica nanoparticles using a mixture of poly (dimethylsiloxane) and diethyl carbonate. Polymers 10 (2), 116.

Rahim Risal, A., Manan, M.A., Yekeen, N., Mohamed Samin, A., Azli, N.B., 2018. Rheological properties of surface-modified nanoparticles-stabilized CO_2 foam. J. Dispers. Sci. Technol. 39 (12), 1767–1779.

Rahmani, O., 2018. Mobility control in carbon dioxide-enhanced oil recovery process using nanoparticle-stabilized foam for carbonate reservoirs. Colloids Surf. A Physicochem. Eng. Asp. 550, 245–255.

Shabib-Asl, A., Ayoub, M.A., Alta'ee, A.F., Saaid, I.B.M., Valentim, P.P.J., 2014. Comprehensive review of foam application during foam assisted water alternating gas (FAWAG) method. Res. J. Appl. Sci. Eng. Technol.

Sivasankar, P., Kumar, G.S., 2019. Influence of bio-clogging induced formation damage on performance of microbial enhanced oil recovery processes. Fuel 236, 100–109.

Sun, J., Jing, J., Brauner, N., Han, L., Ullmann, A., 2018. An oil-tolerant and salt-resistant aqueous foam system for heavy oil transportation. J. Ind. Eng. Chem. 68, 99–108.

Sun, Q., Li, Z., Li, S., Jiang, L., Wang, J., Wang, P., 2014. Utilization of surfactant-stabilized foam for enhanced oil recovery by adding nanoparticles. Energy & Fuels 28 (4), 2384–2394.

Sun, Y., Jia, Z., Yu, B., Zhang, W., Zhang, L., Chen, P., Xu, L., 2024. Research progress of nanoparticles enhanced carbon dioxide foam stability and assisted carbon dioxide storage: a review. Chem. Eng. J. 495, 153177.

Suthar, H., Hingurao, K., Desai, A., Nerurkar, A., 2008. Evaluation of bioemulsifier mediated microbial enhanced oil recovery using sand pack column. J. Microbiol. Methods 75 (2), 225–230.

Takeya, M., Shimokawara, M., Elakneswaran, Y., Nawa, T., Takahashi, S., 2019. Predicting the electrokinetic properties of the crude oil/brine interface for enhanced oil recovery in low salinity water flooding. Fuel 235, 822–831.

Talebian, S.H., Tan, I.M., Sagir, M., Muhammad, M., 2015. Static and dynamic foam/oil interactions: potential of CO_2-philic surfactants as mobility control agents. J. Petrol. Sci. Eng. 135, 118–126.

Tyrode, E., Pizzino, A., Rojas, O.J., 2003. Foamability and foam stability at high pressures and temperatures. I. Instrument validation. Rev. Sci. Instrum. 74 (5), 2925–2932.

Vatanparast, H., Samiee, A., Bahramian, A., Javadi, A., 2017. Surface behavior of hydrophilic silica nanoparticle-SDS surfactant solutions: I. Effect of nanoparticle concentration on foamability and foam stability. Coll. Surf. A: Physicochem. Eng. Asp 513, 430–441.

Wang, X.L., Mei, A., Li, M., Lin, Y., Nan, C.W., 2006. Effect of silane-functionalized mesoporous silica SBA-15 on performance of PEO-based composite polymer electrolytes. Solid State Ionics 177, 1287–1291.

Wei, P., Pu, W., Sun, L., Wang, B., 2017. Research on nitrogen foam for enhancing oil recovery in harsh reservoirs. J. Petrol. Sci. Eng. 157, 27–38.

Worthen, A.J., Bryant, S.L., Huh, C., Johnston, K.P., 2013. Carbon dioxide-in-water foams stabilized with nanoparticles and surfactant acting in synergy. AIChE J. 59 (9), 3490–3501.

Worthen, A.J., Parikh, P.S., Chen, Y., Bryant, S.L., Huh, C., Johnston, K.P., 2014. Carbon dioxide-in-water foams stabilized with a mixture of nanoparticles and surfactant for CO2 storage and utilization applications. Energy Proc. 63, 7929–7938.

Wu, W., Pan, J., 2010. Study on the foamability and its influencing factors of foaming agents in foam-combined flooding. In: 2010 Asia-Pacific Power and Energy Engineering Conference.

Xu, M.H., Cao, Y.Y., Gao, S.G., 2015. Surface modification of nano-silica with silane coupling agent. Key Eng. Mater. 636, 23–27.

Xue, Z., Worthen, A., Qajar, A., Robert, I., Bryant, S.L., Huh, C., Prodanović, M., Johnston, K.P., 2016. Viscosity and stability of ultra-high internal phase CO_2-in-water foams stabilized with surfactants and nanoparticles with or without polyelectrolytes. J. Coll. Interf. Sci. 461, 383–395.

Yekeen, N., Manan, M.A., Idris, A.K., Padmanabhan, E., Junin, R., Samin, A.M., Gbadamosi, Oguamah, I., 2018. A comprehensive review of experimental studies of nanoparticles-stabilized foam for enhanced oil recovery. J. Petrol. Sci. Eng. 164, 43–74.

Zhou, W., Xin, C., Chen, Y., Mouhouadi, R.D., Chen, S., 2023. Nanoparticles for enhancing heavy oil recovery: recent progress, challenges, and future perspectives. Energy & Fuels 37 (12), 8057–8078.

Zhu, D., Wei, L., Wang, B., Feng, Y., 2014. Aqueous hybrids of silica nanoparticles and hydrophobically associating hydrolyzed polyacrylamide used for EOR in high-temperature and high-salinity reservoirs. Energies 7 (6), 3858–3871.